

On computation of diffusion and fibre orientation distribution functions in high angular resolution diffusion imaging

Bartosz P. Neuman¹
bartosz.neuman@nottingham.ac.uk

Christopher Tench²
christopher.tench@nottingham.ac.uk

Li Bai¹
bai.li@nottingham.ac.uk

¹ School of Computer Science
University of Nottingham
Nottingham, UK

² Academic Division of Clinical Neurology
University of Nottingham
Nottingham, UK

Abstract

Diffusion weighted MRI is a non-invasive image technique for obtaining information about the neural architecture of the brain. The measured diffusion signal is highly correlated with the direction of the white matter tracts. Based on the transformed signal (either in the form of orientation distribution function or fibre orientation density) it is possible to estimate the fibre orientations, provided the algorithm used can cope with the noise corrupted diffusion weighted image. This paper reviews the methods used to compute the diffusion and fibre orientation distribution functions.

1 Introduction

Diffusion weighted MRI (DW-MRI) is a non-invasive imaging technique that allows to measure the displacement (diffusion) of water molecules. Applied to the brain, it can be used to recreate the white matter tracts [3], study brain connectivity [26], and detect early changes in the cerebral tissue [4].

Despite intensive research in the DW-MRI, very few methods have been used in clinical applications. One of those that were successful though, was a high angular resolution diffusion imaging (HARDI) protocol [13, 22, 32]. It allows to measure the diffusion signal in a clinically feasible way (*e.g.* provides a good trade-off between the scan time and amount of acquired data). The number of acquired volumes varies on application, but is usually between 30 and 60. Among the methods utilising HARDI there are: generalized diffusion tensor imaging [22], persistent angular structure MRI [17], q-ball imaging (QBI) [31], fibre orientation estimated using continuous axially symmetric tensors [2], and diffusion orientation transform [23].

This paper reviews a QBI and methods related to the computation of diffusion orientation distribution function (ODF) and fibre orientation density (FOD).

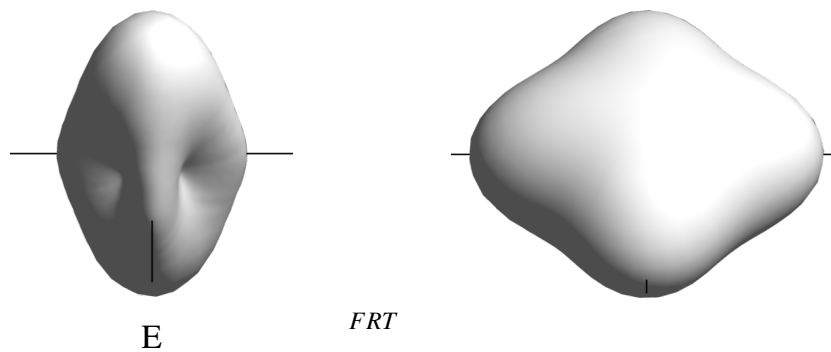


Figure 1: Relationship between the diffusion signal (left) and ODF (right), simulated 90 fibre crossing, 8th order SHS, $b = 3000 \text{ mm}^2 \text{ s}$.

2 Orientation distribution function

In diffusion MRI, the orientation distribution function (ODF) characterizes the 3D distribution of water diffusion, and is necessary to infer the fibre configuration. QBI [31, 33] is a model-independent reconstruction scheme for HARDI. The diffusion ODF is defined as the Funk-Radon transform of the diffusion signal E (see Figure 1 for visual relationship between E and \hat{E}) and can be computed as:

$$\hat{E}(\mathbf{u}) = \int_{\mathbf{q} \perp \mathbf{u}} E(\mathbf{q}) d\mathbf{q} \quad (1)$$

where both \mathbf{u} and \mathbf{q} are unit directions.

The numerical approach to calculate the equator integral required more data than was available from HARDI (since the equator points did not coincide with the diffusion sampling points), and the diffusion signal was interpolated using the spherical radial basis function (sRBF) [12]. Subsequently, Anderson [2], Hess [15, 16], and Descoteaux [9] have independently and in parallel developed an analytical solution for the ODF reconstruction in QBI using spherical harmonic (SH) [21] basis function and Funk–Hecke theorem. First, the diffusion signal is approximated with a truncated spherical harmonic series (SHS) [1]:

$$\hat{E} \approx \sum_{l=0}^n \sum_{m=-l}^l c_{lm} Y_l^m \quad (2)$$

with \hat{E} being the approximation of signal E using n th order SHS, Y_l^m a spherical harmonic function and c_{lm}^m a SH coefficient of order l and band m . The coefficients of the series are found using the spherical harmonic transform (SHT):

$$c_{lm} = \int_0^{2\pi} \int_0^\pi E(\mathbf{d}) Y_l^m(\mathbf{d}) \sin d \, d d \quad (3)$$

In practice, the Equation 3 is rarely used and instead a discrete approximation of the exact solution is found using a linear least squares method:

$$\mathbf{c} = (\mathbf{Y}^T \mathbf{Y})^{-1} \mathbf{Y}^T \mathbf{E} \quad (4)$$

Here \mathbf{Y} is a SH design matrix, and \mathbf{E} is a vector containing the measurements. The diffusion ODF can now be directly estimated from the SH representation of the diffusion signal as:

$$\hat{E}(\mathbf{u}) = \sum_{l=0}^n \sum_{m=-l}^l P_l(\mathbf{u}) c_{lm} Y_l^m \quad (5)$$

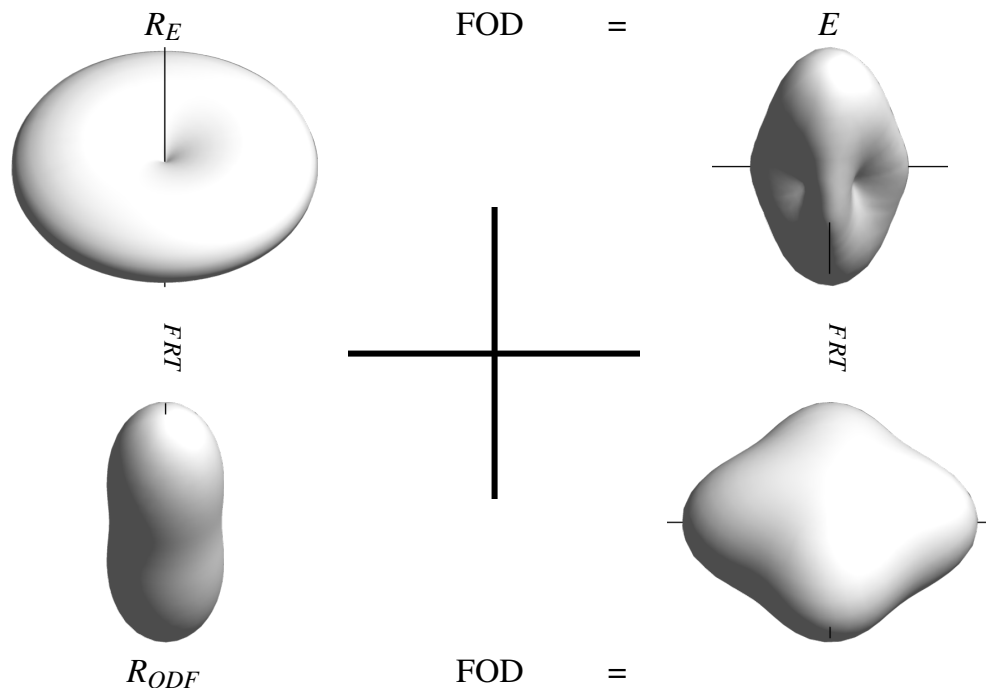


Figure 2: Convolution of a single fibre response with FOD (top – HARDI, bottom – ODF), 8th order SHS and $b = 3000 \text{ mm}^2 \text{ s}$.

with P_l^0 being the associated Legendre function of order l evaluated at 0.

The ODF should be relatively smooth with a few maxima oriented along the direction of underlying fibres. Unfortunately, due to noise the ODF has a lot of sharp spikes and needs to be smoothed. Noise related peaks can be reduced by filtering SH coefficients [27], including a regularization scheme in the signal approximation [10, 16], or by selectively removing the noise-infested basis functions [20]. In the first two cases, the smooth ODF function is produced at the cost of a lower angular resolution.

3 Fibre orientation density

Fibre orientation density (FOD) and fibre orientation distribution function (FODF) is a sharper version of ODF. The spherical deconvolution introduced by Tournier [27] allows to compute FOD directly from HARDI data. The measured signal E is a convolution of unknown FOD F with the signal R_E coming from a single fibre population (Figure 2, top):

$$E = F * R_E \quad (6)$$

The single fibre response R_E is either approximated from the most anisotropic voxels [27] or on a voxel-by-voxel basis [2], and represented by rotational harmonics [14]. Since the SHT is a Fourier transform (on the sphere) the convolution can be efficiently represented with a matrix multiplication, or linear transformation of SH coefficients:

$$f_l^m = c_l^m r_l \quad (7)$$

where f_l^m is a FOD spherical harmonic coefficient of l order and m band, and r_l a rotational harmonic coefficient of a single fibre response R_E .

Ideally, with an infinite SH series the signal would deconvolve to a sum of delta functions oriented along the underlying fibre tracts (Figure 2, FOD). But as the number of samples is

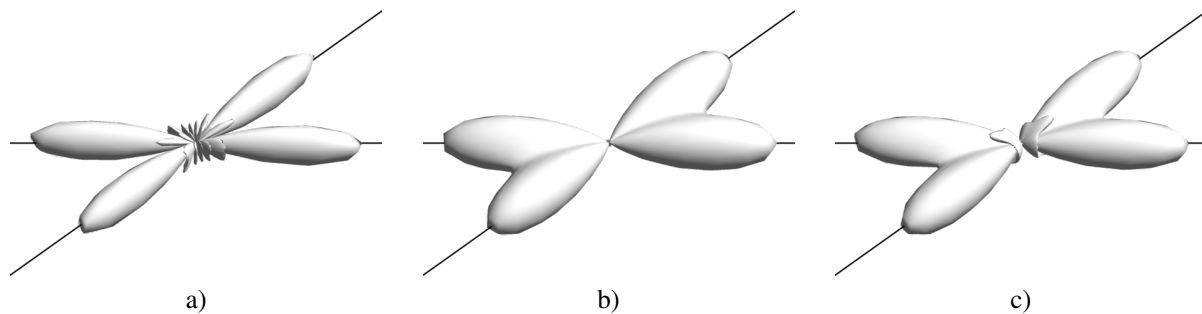


Figure 3: Spherical deconvolution to a delta function (a), cosine power lobe (b) and spherical deconvolution transform (c), simulated 45 fibre crossing, 8th order SHS, $b = 3000 \text{ mm}^2 \text{ s}$.

limited, the series expansion of the signal has to be truncated which results in a smoother FOD and introduces unwanted ringing near the centre of the lobe.

To remove the ringing, and partially reduce the false FOD peaks that are caused by noise Schultz proposed deconvolution using a non-ringing cosine power lobe (\cos^h , where h depends on the size of SHS used) [25]. The resulting FOD is less sharp (Figure 3b) than the classical deconvolution to a delta function (Figure 3a) [27].

Another way of acquiring FOD is based on sharpening the diffusion ODF. Using the same spherical deconvolution method, it is possible to deconvolve a diffusion ODF to FOD using a single fibre response ODF (Figure 2, bottom). Descoteaux provided a formal relationship between ODF and FOD (called fibre ODF, or FODF, as it was derived from ODF) [11]. The method, called spherical deconvolution transform (SDT), like cosine power lobe, produces less sharp but more noise resilient FOD but, unlike cosine power lobe, introduces a regular negative ringing (Figure 3c).

A different approach was sought by Kezele [18], who reconstructed the sharp diffusion ODF by incorporating a spherical wavelet transform into the Funk–Radon transform. Also Tristan-Vega [29, 30] modified the Funk–Radon approximation to the radial integral. By including the Jacobian of the spherical coordinates in FRT he computed a true orientation probability density function (OPDF). Similar approach, but with a different orientation function (both with and without SHT) was proposed by Özarlan [23] in a diffusion orientation transform (DOT).

FOD has the same maxima as ODF, but the function itself should be sharp. The same methods mentioned in the ODF regularization/smoothing can be used to reduce noise related false peaks, but cannot guarantee the non-negativity of the FOD function. The improved deconvolution algorithms proposed by Dell’Acqua [7], Sakaie [24], and Tournier [28] based on iterative approach (with Dell’Acqua using a modified Richardson-Lucy deconvolution [6], and Sakaie and Tournier a spherical deconvolution) address this.

Finally, it is important to note that the spherical harmonic basis functions are globally supported and thus are not well suited to describe sharp FODs. A recent study by Michailovich, in which the HARDI signal (and subsequently ODF) is modelled using multiresolution bases of spherical ridgelets [19] can match the SH-based QBI (45 basis functions) accuracy-wise with just a few basis functions (4 to 8).

4 Examples

Figure 4 shows diffusion signal, ODF, FODF, and two FODs (delta and cosine power lobe) computed over the same region of interest of a whole-brain scan of a healthy male subject.

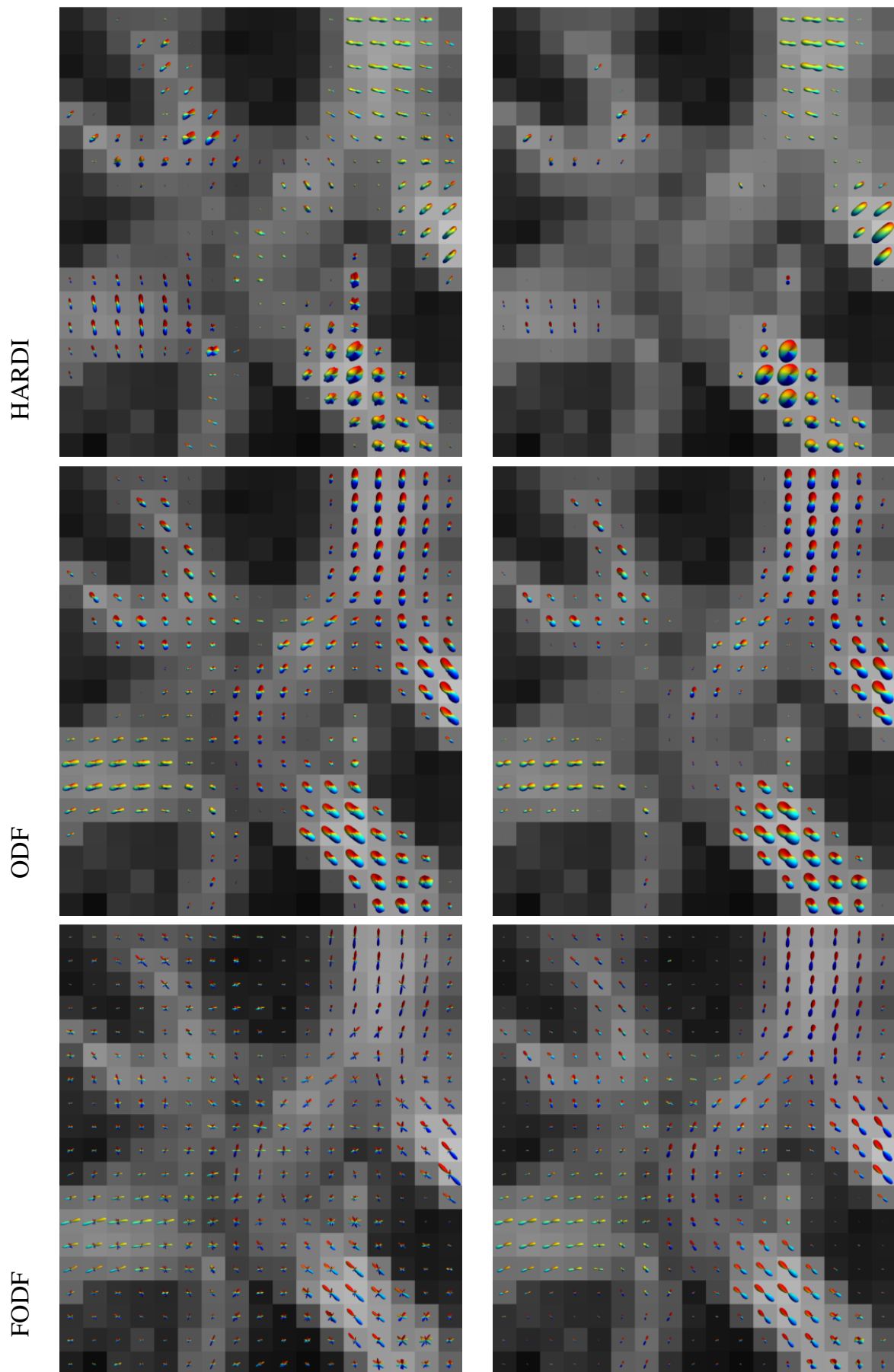


Figure 4

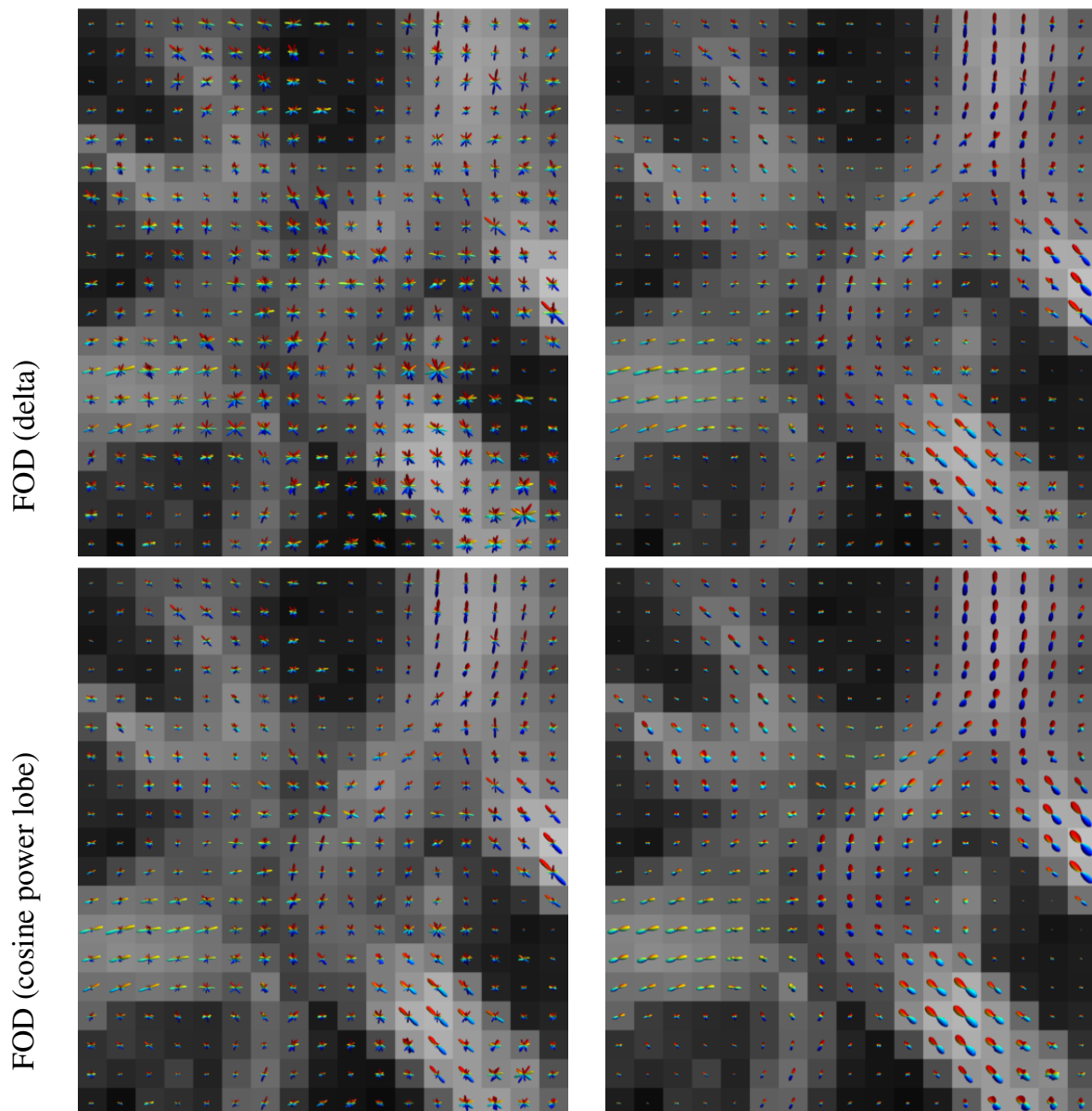


Figure 4: HARDI signal, ODF, FODF, and delta and cosine power lobe FOD profiles plotted over FA of a small region of interest. First column – least squares expansion, second column – regularized expansion using Laplace–Beltrami smoothing operator ($\epsilon = 0.05$).

The image was obtained using a single-shot, spin-echo, echo-planar, diffusion-weighted sequence in a Philips 3T Achieva clinical imaging system¹. Both least squares and smoothed (using Tikhonov regularization with Laplace–Beltrami operator [8]) profiles are provided.

5 Conclusion

Every year new papers related to the processing of diffusion weighted images are published. Methods for computing ODF and FOD has been studied for over 10 years now. This review summarises recent development and provides some insight into the current state of the art in

¹Acquisition matrix 112x112 with in-plane resolution $2 \times 2 \text{ mm}^2$; 52 slices with a thickness of 2 mm; $b = 3000 \text{ s/mm}^2$; $TE = 72 \text{ ms}$; $TR = 15292 \text{ ms}$; 61 evenly spaced diffusion weighting directions [5]; six $b = 0 \text{ s/mm}^2$ images acquired and averaged

that broad field. Despite all the work summarized here, the ODF and FOD computation has not yet reached its maturity and still offers a great opportunity for research.

References

- [1] D.C. Alexander, G.J. Barker, and S.R. Arridge. Detection and modeling of non-Gaussian apparent diffusion coefficient profiles in human brain data. *Magnetic Resonance in Medicine*, 48:331–340, 2002.
- [2] A.W. Anderson. Measurement of fiber orientation distributions using high angular resolution diffusion imaging. *Magnetic Resonance in Medicine*, 54:1194–1206, 2005.
- [3] P.J. Basser, S. Pajevic, C. Pierpaoli, J. Duda, and A. Aldroubi. In vivo fiber tractography using DT-MRI data. *Magnetic Resonance in Medicine*, 44:625–632, 2000.
- [4] D.L. Bihan. Molecular diffusion, tissue microdynamics and microstructure. *NMR in Biomedicine*, 8:375–386, 1995.
- [5] P.A. Cook, M. Symms, P.A. Boulby, and Alexander D.C. Optimal acquisition orders of diffusion-weighted MRI measurements. *Journal of Magnetic Resonance*, 25:1051–1058, 2007.
- [6] M.E. Daube-Witherspoon and G. Muehllehner. An iterative image space reconstruction algorithm suitable for volume ECT. *IEEE Transactions on Medical Imaging*, 5:61–66, 1986.
- [7] F. Dell’Acqua, G. Rizzo, P. Scifo, R.A. Clarke, G. Scotti, and F. Fazio. A model-based deconvolution approach to solve fiber crossing in diffusion-weighted MR imaging. *IEEE Transactions on Biomedical Engineering*, 54:462–472, 2007.
- [8] M. Descoteaux, E. Angelino, S. Fitzgibbons, and R. Deriche. Apparent diffusion coefficients from high angular resolution diffusion imaging: estimation and applications. *Magnetic Resonance in Medicine*, 56:395–410, 2006.
- [9] M. Descoteaux, E. Angelino, S. Fitzgibbons, and R. Deriche. A fast and robust ODF estimation algorithm in q-ball imaging. In *IEEE International Symposium on Biomedical Imaging: From Nano to Macro*, 2006.
- [10] M. Descoteaux, E. Angelino, S. Fitzgibbons, and R. Deriche. Regularized, fast, and robust analytical q-ball imaging. *Magnetic Resonance in Medicine*, 58:497–510, 2007.
- [11] M. Descoteaux, R. Deriche, T.R. Knosche, and A. Anwender. Deterministic and probabilistic tractography based on complex fibre orientation distributions. *IEEE Transactions on Medical Imaging*, 28:269–286, 2009.
- [12] G. E. Fasshauer and L. L. Schumaker. Scattered data fitting on the sphere. In *International Conference on Mathematical Methods for Curves and Surfaces II*, 1998.
- [13] L.R. Frank. Anisotropy in high angular resolution diffusion-weighted MRI. *Magnetic Resonance in Medicine*, 45:935–939, 2001.
- [14] D.M. Healy, H. Hendriks, and P.T. Kim. Spherical deconvolution. *Journal of Multivariate Analysis*, 67:1–22, 1998.
- [15] C.P. Hess, P. Mukherjee, E.T. Han, D. Xu, and D.B. Vigneron. A spherical harmonic approach to q-ball imaging. In *International Society for Magnetic Resonance in Medicine*, 2005.
- [16] C.P. Hess, P. Mukherjee, E.T. Han, D. Xu, and D.B. Vigneron. Q-ball reconstruction of multimodal fiber orientations using the spherical harmonic basis. *Magnetic Resonance in Medicine*, 56:104–117, 2006.

- [17] K.M. Jansons and D.C. Alexander. Persistent angular structure: new insights from diffusion magnetic resonance imaging data. *Inverse Problems*, 19:1031, 2003.
- [18] I. Kezele, M. Descoteaux, C. Poupon, F. Poupon, and J.F. Mangin. Spherical wavelet transform for ODF sharpening. *Medical Image Analysis*, 14:332–342, 2010.
- [19] O. Michailovich and Y. Rathi. On approximation of orientation distributions by means of spherical ridgelets. *IEEE Transactions on Image Processing*, 19:461–477, 2010.
- [20] B.P. Neuman, L. Bai, and C. Tench. Reliably estimating the diffusion orientation distribution function from high angular resolution diffusion imaging data. In *Medical Image Understanding and Analysis*, 2011.
- [21] A.F. Nikiforov, V.B. Uvarov, and R.P. Boas. *Special functions of mathematical physics*. Birkhäuser BaselBoston, 1988.
- [22] E. Özarslan and T.H. Mareci. Generalized diffusion tensor imaging and analytical relationships between diffusion tensor imaging and high angular resolution diffusion imaging. *Magnetic Resonance in Medicine*, 50:955–965, 2003.
- [23] E. Özarslan, T.M. Shepherd, B.C. Vemuri, S.J. Blackband, and T.H. Mareci. Resolution of complex tissue microarchitecture using the diffusion orientation transform (DOT). *NeuroImage*, 31:1086–1103, 2006.
- [24] K.E. Sakaie and M.J. Lowe. An objective method for regularization of fiber orientation distributions derived from diffusion-weighted MRI. *NeuroImage*, 34:169–176, 2007.
- [25] T. Schultz and H.-P. Seidel. Estimating crossing fibers: A tensor decomposition approach. *IEEE Transactions on Visualization and Computer Graphics*, 14:1635–1642, 2008.
- [26] S.N. Sotiropoulos, L. Bai, and C.R. Tench. Fuzzy anatomical connectedness of the brain using single and multiple fibre orientations estimated from diffusion MRI. *Computerized Medical Imaging and Graphics*, 34:504–513, 2010.
- [27] J.D. Tournier, F. Calamante, D.G. Gadian, and A. Connelly. Direct estimation of the fiber orientation density function from diffusion-weighted MRI data using spherical deconvolution. *NeuroImage*, 23:1176–1185, 2004.
- [28] J.D. Tournier, F. Calamante, and A. Connelly. Robust determination of the fibre orientation distribution in diffusion MRI: non-negativity constrained super-resolved spherical deconvolution. *NeuroImage*, 35:1459–1472, 2007.
- [29] A. Tristán-Vega, C.F. Westin, and S. Aja-Fernández. Estimation of fiber orientation probability density functions in high angular resolution diffusion imaging. *NeuroImage*, 47:638–650, 2009.
- [30] A. Tristán-Vega, C.F. Westin, et al. A new methodology for the estimation of fiber populations in the white matter of the brain with the Funk-Radon transform. *NeuroImage*, 49:1301–1315, 2010.
- [31] D.S. Tuch. Q-ball imaging. *Magnetic Resonance in Medicine*, 52:1358–1372, 2004.
- [32] D.S. Tuch, T.G. Reese, M.R. Wiegell, N. Makris, J.W. Belliveau, and V.J. Wedeen. High angular resolution diffusion imaging reveals intravoxel white matter fiber heterogeneity. *Magnetic Resonance in Medicine*, 48:577–582, 2002.
- [33] D.S. Tuch, T.G. Reese, M.R. Wiegell, and V.J. Wedeen. Diffusion MRI of complex neural architecture. *Neuron*, 40:885–895, 2003.